CHEMICAL EXCHANGE SATURATION TRANSFER (CEST) IMAGING USING INTERLEAVED BALANCED STEADY STATE FREE PRECESSION (SSFP)

Zhongliang Zu[1,2], Ke Li[1,2], Richard Dortch[1,2], Seth Smith[1,2], Mark D Does[1,2], John Gore[1,2], and Daniel Gochberg[1,2]
[1]*Institute of Imaging Science, Vanderbilt University, Nashville, TN, United States,* [2]*Department of Radiology, Vanderbilt University, Nashville, TN, United States*

Introduction: Chemical exchange saturation transfer (CEST) imaging is based on measuring water signal attenuation caused by the exchange of magnetization between radio frequency labeled solute protons and water protons. It has found significant applications in imaging stroke and cancer. Conventionally, a long saturation block (typically several seconds of continuous wave or pulsed irradiation) is performed before the acquisition to label the solute protons. This saturation block and acquisition are then repeated several times in order to fill *k*-space, resulting in long scan times that limit CEST imaging in clinical applications, especially at high-resolution. Here we present a new CEST imaging method using interleaved balanced steady state free precession (SSFP) acquisitions (named SSFP-CEST) to shorten imaging time.

Methods:

Pulsed Sequence: Balanced SSFP is a highly SNR-efficient sequence for high spatial-resolution imaging. However, bright signal from lipid obscures visualization of other structures. To suppress the lipid signal, frequency-selective fat-suppressed SSFP has been proposed. In this approach, magnetization is longitudinally stored after an $\alpha/2$ flip-back pulse, which provides an interruption of the steady state and makes insertion of a frequency selective suppression pulse possible [1]. In this study, we investigate a modification of the fat-suppression SSFP sequence where the fat-suppression pulse is replaced by a solute saturating pulse. By performing these saturating pulses on solutes, instead of lipids, bulk water signal is attenuated through magnetization exchange. The resulting interleaved SSFP data acquisition facilitates rapid high-resolution CEST imaging.

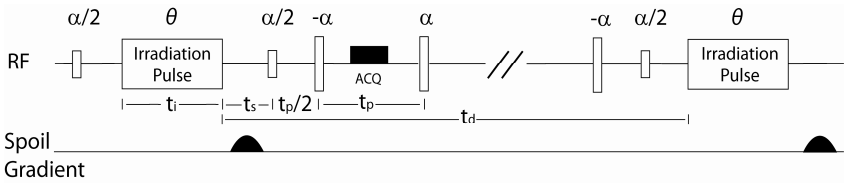

Fig. 1: Schematic of one unit of SSFP-CEST sequence. The unit repeats without data acquisition for a few seconds to enhance CEST contrast forming the saturation block, and then repeats for acquisition until the *k*-space is filled.

A SSFP-CEST pulse sequence was implemented on a Philips Achieva 3T scanner (Fig. 1). In detail, a Gaussian off-resonance saturation pulse with duration t_i and flip angle θ, followed by a spoiler gradient with duration t_s, is interleaved periodically into a train of alternating $\pm\alpha$ on-resonance sinc excitation pulses. Spoiler gradients were applied after the irradiation pulse to avoid buildup of transverse magnetization. Two $\alpha/2$ pulses are also applied before and after the irradiation pulse as in a conventional fat-saturated SSFP sequence. Likewise, data are acquired at $t_E = t_p/2$ after an excitation pulse. All imaging gradients applied on three axes are fully rewound. Dummy scans are applied before data acquisition to allow the spin system to reach dynamic equilibrium.

Data Analysis: MTR_{asym} is defined to be the difference between the signals when applying positive ($S(+)$) and negative ($S(-)$) offset irradiations divided by the non-irradiated control signal (S_0) (Eq. (1)). For SSFP-CEST, S_0 is acquired by setting the irradiation power to zero.

$$MTR_{asym} = (S(+) - S(-))/S_0 \qquad (1)$$

Data Acquisition: SSFP-CEST experiments were performed on a creatine phantom (50 mM Creatine plus 3% agarose solution (w/w), pH 7.0) on a Philips 3T MR scanner with body coil excitation and a 32 element head coil for reception. Z-spectra from -500 Hz to 500 Hz (around - 4 ppm to + 4 ppm at 3 T) with an interval of 50 Hz (around 0.4 ppm at 3 T) were acquired. θ and α were set to be 180° and 15°. 8 excitation pulses and one solute irradiation pulse were performed in each segment. t_i, t_s, and t_p were set to be 30 ms, 7 ms, and 3.4 ms, respectively, with a corresponding t_d of ~40 ms. 8 s of dummy scans were incorporated to reach steady state. Images had a field of view (FOV) of 180 mm × 180 mm, voxel size 2 mm × 2 mm, slice thickness of 5 mm, and 1 average. Pulsed-CEST [2] experiments with a SE-EPI acquisition (6 *k*-space shots) were also performed with the same geometry and sequence parameters (θ, t_i, and t_d) for comparison with SSFP-CEST. Total acquisition times for SSFP-CEST and pulsed-CEST were about 3.2 minutes and 19.1 minutes, respectively.

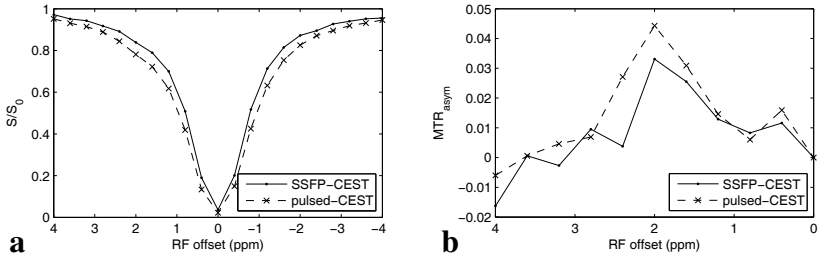

Fig. 2: Z-spectrum (a) and MTR_{asym} (b) with SSFP- and pulsed-CEST.

Results: Fig. 2 compares z-spectra (a) and MTR_{asym} (b) using the SSFP-CEST and pulsed-CEST sequences. It was found that the SSFP-CEST MTR_{asym} at the creatine resonance (3.3%) is about 75% of that of pulsed-CEST (4.4%), while the variation over the sample was 3 times greater. Hence, while the total acquisition time of conventional pulsed-CEST is roughly 6 times longer than SSFP-CEST, it still has ~60% greater SNR efficiency for the particular acquisition described above. Therefore, our initial results indicate that the primary application of SSFP-CEST is likely rapid high-resolution imaging, though perhaps not with the greatest SNR efficiency. All results thus far are based on very limited initial data.

Discussion: In this work, we showed how an SSFP sequence with interspersed solute saturation pulses gives similar results to conventional EPI based CEST sequences, but in considerably less time, at least for high-resolution imaging. This method is directly applicable to systems equipped with a generic SSFP imaging sequence modified with only modest pulse programming.

References:

[1] Scheffler, K. et al., *Magn. Reson. Med.* 45, 1075 (2001) [2] Sun, P. Z. et al., *Magn. Reson. Med.* 60, 834 (2008)

Acknowledgements: This research is supported by Vanderbilt Bridge Funding and NIH EB001744.